UDC 553.3:622.73:539.42 DOI: https://doi.org/10.15407/geotm2026.176.179

***Valerii Ishkov*[1,2]*, https://orcid.org/0000-0002-3987-208X
***Oleksandr Berezniak*[1]*, https://orcid.org/0000-0003-1807-4828
***Yevhen Kozii*[2,3]*, https://orcid.org/0000-0002-2167-6224
***Pavlo Pashchenko*[2]*, https://orcid.org/0000-0001-7217-645X
***Mykola Kozar*[4]*, https://orcid.org/0000-0001-9070-4121

[1]*Dnipro University of Technology of MSE of Ukraine, Dnipro, Ukraine*
[2]*M.S. Poliakov Institute of Geotechnical Mechanics of the National Academy of Sciences of Ukraine, Dnipro, Ukraine*
[3]*Technical University "Metinvest Polytechnic", Zaporizhzhia, Ukraine*
[4]*M.P. Semenenko Institute of Geochemistry, Mineralogy and Ore Formation of the National Academy of Sciences of Ukraine, Kyiv, Ukraine*
**Corresponding author e-mail:* ishwishw37@gmail.com

EVOLUTION OF MICROCRACKING IN PR_1SX^1F IRON QUARTZITES (NOVOKRYVORIZKE DEPOSIT) DURING COMMINUTION

Abstract. The study aims to establish the regularities of multiscale hierarchical reorganization of the microcrack network in PR_1sx^1f banded iron formation during the complete technological cycle of crushing and wet ball grinding, providing a quantitative interpretation of stage-specific transitions in defect generation mechanisms.

The research is based on comprehensive petrographic and quantitative microstructural analysis of iron quartzites sampled after successive stages of dry crushing and wet grinding. Measurements were performed using a polarizing microscope (Polam R-312) and an inverted metallographic microscope (LMM 1400) at fixed magnifications to ensure statistical reliability. Integral descriptors of microcracking were calculated, including the Linear Microcrack Density Coefficient, the Microcrack Density Coefficient, the Hierarchical Reorganization Coefficient (*Kier*), and the Scale Redistribution Index (*Im*). Statistical analysis of microcrack length distributions was carried out to evaluate changes in defect scale and spatial organization.

The findings demonstrate that the evolution of microcracking has a pronounced multilevel hierarchical character. A monotonic decrease in characteristic microcrack length is accompanied by a multiple increase in crack density, indicating a transition from localized crack growth to intensive initiation and interaction of short-scale defects. Stage-to-stage analysis using Kier reveals alternation between balanced crack growth and predominance of crack initiation, reflecting nonlinear restructuring of the defect field. The quasi-exponential growth of *Im* confirms progressive scale redistribution toward ultrashort microcracks and the formation of a highly dense hierarchical defect structure.

The results identify structural prerequisites for enhanced material reactivity and improved mineral liberation during beneficiation. The formation of a dense network of ultrashort microcracks creates favourable conditions for magnetite liberation within the quartz matrix and for optimizing comminution regimes.

The originality of the study lies in the quantitative description of stage-specific transitions in defect generation mechanisms and in the introduction of complementary diagnostic indicators (*Kier* and *Im*) that integrate local transition behaviour with cumulative scale redistribution of the microcrack system.

Keywords: banded iron formation; microcrack evolution; hierarchical defect structure; multistage comminution; mineral liberation.

1. Introduction

The Novokryvorizke iron quartzite deposit is located within the Southern structural-tectonic region of the Kryvyi Rih Basin, approximately 4 km south of the city of Kryvyi Rih. The southern part of the deposit, adjacent to the core of the Inhuletska anticline, is currently mined by Open Pit No. 2-bis. The geological structure of the area comprises metamorphic rocks of the Kryvyi Rih Series (Paleoproterozoic), which form the ore-bearing sequence of the Kryvyi Rih iron ore basin.

The first iron-bearing horizon (PR_1sx^1f) is represented by magnetite, silicate-carbonate-magnetite, and carbonate-magnetite quartzites with medium- to coarse-banded textures. The main rock-forming minerals are magnetite, quartz, amphibole (cummingtonite), chlorite, biotite, and carbonates. The heterogeneity of the

Received: 18.12.2025 Accepted: 11.02.2026 Available online: 31.03.2026

magnetite–quartz system, caused by the contrast in elastic and strength properties of the mineral phases, generates local stress fields at interphase boundaries and creates conditions for the development of a complex multilevel fracture network.

The problem of microcrack evolution in heterogeneous brittle rocks is inherently interdisciplinary and integrates concepts from fracture mechanics, micromechanics of defect generation, and comminution engineering [1, 2]. Fundamental studies in rock mechanics have demonstrated that failure occurs through nucleation, growth, and coalescence of microcracks, leading to the formation of a hierarchical defect system [3-5]. Experimental investigations of crystalline rock deformation indicate that increasing load intensity causes a transition from localized growth of individual cracks to the massive generation of short-scale defects [4, 6]. These regularities form the basis of modern models of brittle particle breakage during crushing and grinding processes [7, 8]. However, the application of such models to heterogeneous magnetite–quartz systems requires dedicated quantitative studies that take into account their specific textural and mineralogical characteristics.

At the same time, most existing studies have been conducted either on relatively homogeneous rocks or under laboratory loading conditions, whereas real technological comminution processes are characterized by multistage sequences and varying stress regimes. In mineral processing, it is widely recognized that the efficiency of valuable mineral liberation depends not only on the particle-size distribution of the products but also on the evolution of fracture networks along interphase boundaries [9-12], which directly affects the efficiency and optimization of comminution circuits [13]. Recent studies on comminution modelling and microstructural control of fracture emphasize the importance of accounting for inherited defect structures and the multiscale organization of crack fields [14-16]. Modern investigations also demonstrate the possibility of intensifying crack generation through thermal and electrophysical effects, particularly microwave treatment and high-voltage pulse discharge, which promote the development of defect structures in rocks [17-19].

Despite this, quantitative studies of the multistage evolution of microcracking in iron quartzites from different stratigraphic horizons of the Kryvyi Rih Basin remain limited. In particular, stage-specific transitions in defect generation mechanisms throughout the complete technological processing cycle-from dry crushing to wet ball grinding-remain insufficiently investigated. This highlights the need for integrated quantitative approaches capable of capturing both the structural and scale-related aspects of microcrack evolution in heterogeneous ore systems.

The object of this study is iron quartzites of the PR_1sx^1f horizon of the Novokryvorizke deposit. The subject of the study is the transformation patterns of their microcrack structure during sequential comminution.

The aim of this work is to identify the patterns of multiscale hierarchical reorganization of the fracture network in iron quartzites of the PR_1sx^1f horizon during the complete technological cycle of crushing and grinding and to provide a quantitative interpretation of stage-specific changes in defect generation mechanisms.

2. Methods

The study of microcrack transformation in iron quartzites during technological comminution was carried out using an integrated mineralogical and petrographic approach combined with quantitative microstructural analysis. The methodology was aimed not only at recording changes in individual parameters of the fracture system but also at identifying patterns of multiscale defect redistribution and transitions between different failure regimes.

To trace the evolution of the defect structure, a complete series of thin sections and polished sections was prepared from the initial sample (V) and from material collected after each successive comminution stage. The sampling scheme included three stages of dry crushing (C1, C2, C3) and three stages of wet ball grinding (G1, G2, G3), allowing the material state to be recorded at all key stages of the technological cycle. All specimens were prepared using a standardized surface preparation procedure with consistent grinding and polishing conditions, minimizing the risk of artefact crack formation and ensuring the reliability of inter-stage comparisons. Such an approach ensures comparability of microstructural parameters obtained at different stages of comminution. It also minimizes methodological uncertainties associated with sample preparation and measurement conditions.

Petrographic examinations were performed using a polarizing binocular microscope (Polam R-312) and an inverted metallographic microscope (LMM 1400) at fixed magnifications identical for all processing stages. To achieve complete visualization of the fracture network, a combination of transmitted and reflected light modes was employed, enabling identification of defects both in the quartz matrix and in magnetite, as well as along interphase boundaries. Only inherited and technologically induced microcracks were considered in the calculations, while cleavage cracks were excluded from the analysis.

The intensity of defect generation was evaluated using two integral parameters. The linear microcrack density coefficient was defined as the ratio of the total length of recorded microcracks to the analysis area:

$$Ktr.l = \frac{L}{S}, \quad (1)$$

where L is the total length of microcracks and S is the measurement area.

The microcrack density coefficient was calculated as the number of individual cracks per unit area:

$$Ktr.d = \frac{N}{S}, \quad (2)$$

where N is the number of microcracks within area S. The parallel use of these coefficients enabled differentiation between the processes of elongation of existing cracks and initiation of new defects.

For each processing stage, the principal statistical characteristics of microcrack length distributions were determined, including the arithmetic mean, median, and mode. The distribution shape was preliminarily assessed using the Shapiro–Wilk test. In cases of statistically significant deviation from normality, nonparametric tests (Mann–Whitney for pairwise comparisons and Kruskal–Wallis for multiple comparisons) were applied. The level of statistical significance was set at $p<0.05$, ensuring reliable interpretation of differences between processing stages.

To quantitatively assess changes in the dominant fracture mechanism and the degree of hierarchical reorganization of the crack network, two additional diagnostic indicators were introduced. The hierarchical reorganization coefficient K_{ier} was determined for each transition between successive stages as:

$$K_{ier}^{(i)} = \frac{(K_{tr.d}^{i} / K_{tr.d}^{i-1})}{(K_{tr.l}^{i} / K_{tr.l}^{i-1})}, \qquad (3)$$

where i is the current stage and $i-1$ is the preceding stage. Values of $K_{ier}^{(i)} < 1$ indicate dominance of the development of existing cracks, $K_{ier}^{(i)} \approx 1$ correspond to a balanced regime of crack growth and initiation, whereas $K_{ier}^{(i)} > 1$indicate predominance of new defect generation and transition to hierarchical defect development.

The scale redistribution index I_m was defined as:

$$\mathrm{Im} = \frac{Ktr.d}{l}, \qquad (4)$$

where $\bar{l}$ is the mean microcrack length. This parameter reflects the cumulative effect of fragmentation of the crack network and is used to assess the depth of transition of the system into a fine-scale hierarchical regime. Unlike the local parameter K_{ier}, which characterizes the fracture mechanism at individual transitions, the index I_m serves as an integral indicator of multiscale reorganization of the defect field throughout the entire processing cycle.

Interpretation of the obtained results was performed taking into account the hierarchical nature of fracture in brittle heterogeneous systems, according to which part of the longer microcracks coalesce during crushing and transition to meso- and macrolevels, whereas the observed field becomes dominated by the generation of new short-scale defects. This approach allowed the transformation of microcracking to be considered not as a simple accumulation of damage but as a sequential transition of the system between different regimes of defect-structure self-organization.

Thus, the proposed methodology combines parametric analysis with a conceptual interpretation of multiscale redistribution of the crack structure, allowing the transformation of microcracking in iron quartzites of the PR_1sx^1f horizon to be interpreted as a sequential transition between regimes of defect-field self-organization during technological comminution.

3. Results and Discussion

The results of quantitative microstructural analysis (Table 1; Fig. 1) demonstrate a sequential transformation of microcracking in iron quartzites of the PR_1sx^1f horizon during technological comminution.

Table 1 – Changes in microcrack parameters of PR_1sx^1f banded iron formation during crushing and grinding

Processing stages	Parameters				
	Average length of microcracks (mm)	Median length of microcracks (mm)	Modal length of microcracks (mm)	Linear microcracking coefficient, $K_{tr.l}$	Microcrack density coefficient, $K_{tr.d}$
V	0.2965	0.2963	0.2966	47.5138	2.1250
C1	0.2313 (-22%)	0.2193 (-26%)	0.2284 (-23%)	134.4641 (+210%)	6.2688 (+195%)
C2	0.2135 (-28%)	0.1926 (-35%)	0.2047 (-31%)	240.8950 (+327%)	11.3263 (+433%)
C3	0.1868 (-37%)	0.1719 (-42%)	0.1809 (-39%)	399.5911 (+448%)	19.4438 (+815%)
G1	0.1038 (-65%)	0.0770 (-74%)	0.0949 (-68%)	696.0772 (+649%)	33.1713 (+1461%)
G2	0.0623 (-79%)	0.0415 (-86%)	0.0475 (-84%)	1222.0549 (+827%)	49.8738 (+2247%)
G3	0.0356 (-88%)	0.0148 (-95%)	0.0267 (-91%)	1826.4305 (+1042%)	78.3063 (+3585%)

Note: V – initial sample; C1–C3 – crushing stages; G1–G3 – grinding stages.

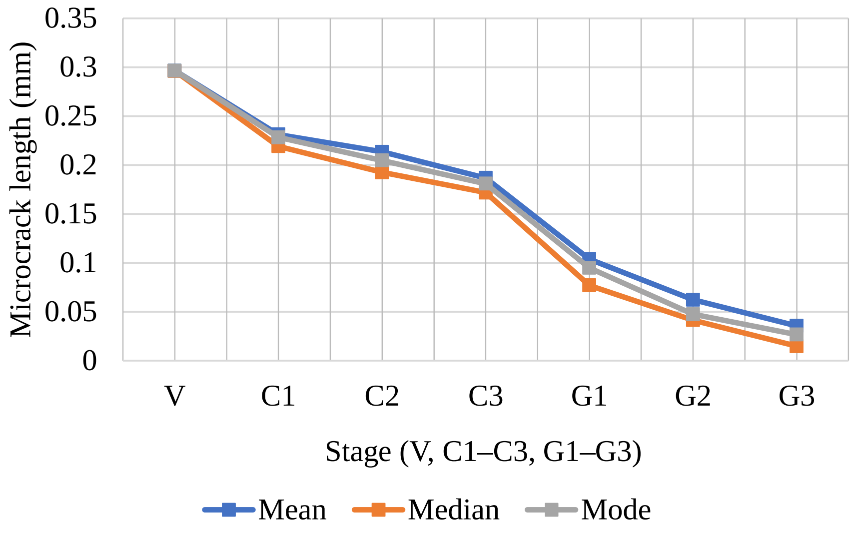

Figure 1 – Statistical parameters of microcrack length distribution (mean, median and mode) at different stages of comminution

The length characteristics show a monotonic decrease in the characteristic scale of microcracks from the initial state to the third stage of wet grinding. The mean microcrack length decreases from 0.2965 mm in the initial state to 0.1868 mm at stage C3 (–37% relative to V) and to 0.0356 mm at stage G3 (–88% relative to V). A similar trend is observed for the median and modal values, indicating a systematic shift of the length distribution toward short-scale defects.

The integral microcracking coefficients exhibit the opposite trend. The linear microcrack density coefficient increases from 47.51 in the initial state to 399.59 at stage C3 (+741% relative to V) and to 1826.43 at stage G3 (+3743% relative to V). The microcrack density coefficient increases from 2.13 to 19.44 at stage C3 (+815% relative to V) and to 78.31 at stage G3 (+3585% relative to V). Thus, the reduction in characteristic crack scale is accompanied by a multiple increase in the saturation of the defect field.

The local hierarchical reorganization coefficient K_{ier} reflects changes in the ratio between the growth rates of crack density and total crack length at transitions between successive stages (Table 2). At the transitions V→C1, C1→C2, and C2→C3, its values are close to unity (1.01–1.04), corresponding to a balanced regime of crack growth and initiation. At the transition C3→G1 the coefficient decreases to 0.98, and at G1→G2 to 0.86, reflecting the predominance of propagation of existing cracks. At the stage G2→G3, K_{ier} again exceeds unity (1.05), indicating a renewed predominance of new microcrack initiation.

Table 2 – Local hierarchical reorganization coefficient $K_{ier}$for stage transitions (PR_1sx^1f horizon)

Stage transition	$\Delta K_{tr.d}$, %	$\Delta K_{tr.l}$, %	K_{ier}	Interpretation
V → C1	+195.00	+183.00	1.04	Nearly balanced regime
C1 → C2	+80.70	+79.20	1.01	Balanced crack growth and initiation
C2 → C3	+71.70	+65.90	1.04	Moderate predominance of initiation
C3 → G1	+70.60	+74.20	0.98	Slight predominance of crack elongation
G1 → G2	+50.40	+75.60	0.86	Dominance of propagation of existing cracks
G2 → G3	+57.00	+49.50	1.05	Increased generation of new defects

The scale redistribution index I_m demonstrates quasi-exponential growth throughout the entire processing cycle (Table 3). While its value in the initial state is 7.17, it increases to 104.10 at stage C3 (14.5× relative to V) and to 2199.62 at stage G3 (306.8×). This indicates progressive multiscale redistribution of defects toward ultra-short microcracks.

Thus, it has been established that during the comminution process a simultaneous decrease in characteristic crack length and a multiple increase in their number and total length occur, indicating a transition of the system to a multilevel regime of defect generation.

The obtained results indicate that the evolution of microcracking in iron quartzites during the comminution cycle occurs through sequential reorganization of the fracture network, where an increase in its saturation is combined with a shift in the length distribution toward short-scale defects. Such a pattern of changes corresponds to the concepts of brittle fracture mechanics concerning cascade microcrack generation and self-organization of the defect field under loading [1, 2]. Within micromechanical approaches, this is interpreted as a transition from localized growth of individual cracks to their massive initiation and interaction [3, 4].

Table 3 – Scale redistribution index I_m across processing stages (PR_1sx^1f horizon)

Processing stage	$K_{tr.d}$	Mean crack length (mm)	I_m	Relative increase
V	2.13	0.30	7.17	1.00×
C1	6.27	0.23	27.10	3.78×
C2	11.33	0.21	53.07	7.40×
C3	19.44	0.19	104.10	14.52×
G1	33.17	0.10	319.57	44.57×
G2	49.87	0.06	800.54	111.65×
G3	78.31	0.04	2199.62	306.78×

Comparison of length characteristics (Fig. 1) with integral microcracking coefficients (Fig. 2) shows that a sharp reduction in mean crack length at the later stages is accompanied by an avalanche-like increase in their density. This dynamic is consistent with the results of experimental studies on crystalline rock deformation, which have established a shift from dominance of crack elongation to massive crack generation with increasing load intensity [4, 6].

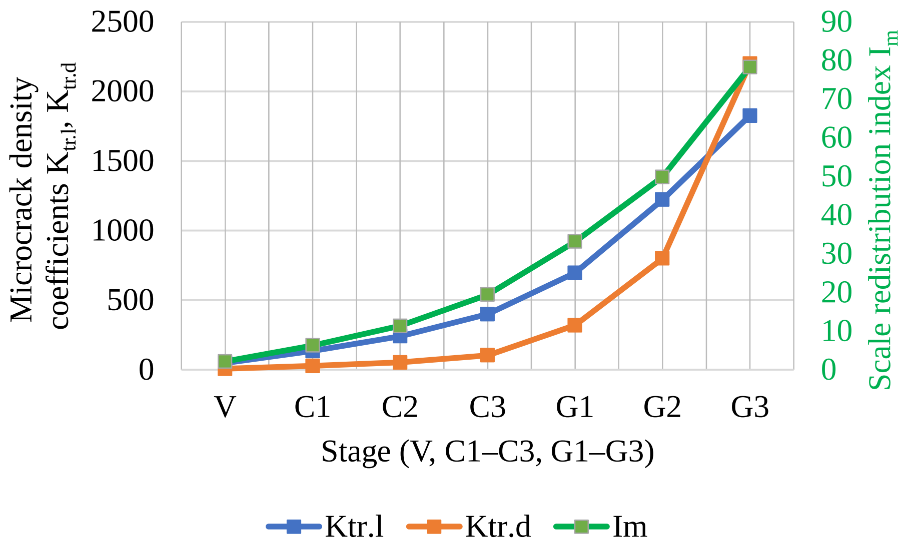

Figure 2 – Evolution of microcrack density coefficients $K_{tr.l}$, $K_{tr.d}$ and the scale redistribution index I_m during successive stages of comminution

Analysis of the local coefficient K_{ier} allows specification of the stage-specific features of this transition. During the crushing stages, the coefficient values are close to unity, corresponding to a balanced regime of crack growth and initiation. Such a regime is characteristic of brittle particle fragmentation under impact loading conditions [7, 8]. The transition to wet ball grinding is accompanied by a change in the ratio of processes: initially, coalescence and propagation of already formed cracks dominate, while at the final stage, the predominance of new defect initiation is restored. This nonlinear dynamics is consistent with modern models of subcritical microcracking, which describe alternation between stable growth and avalanche-like defect generation [16, 20].

The scale redistribution index I_m reflects the cumulative aspect of this reorganization. Its quasi-exponential growth indicates a gradual loss by the system of a characteristic "dominant" crack scale and the acquisition of features of scale invariance. Similar multilevel fracture structures have been described in studies devoted to fractal characteristics of fracture and cataclastic media [21, 22]. Although direct fractal analysis was not performed in this work, the behavior of I_m is consistent with the formation of a hierarchical, statistically self-similar defect network.

The revealed regularities have direct technological significance, which aligns with modern approaches to optimizing the processing of complex ore systems [23]. According to the principles of applied mineralogy and the theory of mineral liberation [9-11], the efficiency of beneficiation processes is determined not only by product particle size distribution but also by the pattern of mineral liberation along interphase boundaries. The formation of an ultra-dense network of ultrashort microcracks creates structural prerequisites for enhancing the material's reactivity and improving the conditions for magnetite liberation within the quartz matrix. Such a role of microstructure in comminution processes is also emphasized in recent review studies [16].

4. Conclusions

1**.** Comminution of PR_1sx^1f banded iron formation during crushing and wet ball grinding represents a multistage process of hierarchical reorganization of the defect field, characterized by a transition from balanced crack growth and initiation to the formation of an extremely dense network of ultrashort microcracks.

2. Quantitative analysis revealed a systematic decrease in characteristic microcrack length accompanied by a sharp increase in crack density, indicating a transition from localized defect growth to a regime of intensive crack generation and interaction.

3. The combined application of the hierarchical reorganization coefficient K_{ier} and the scale redistribution index I_m provides a quantitative framework for identifying stage-specific transitions in defect generation mechanisms and for assessing the depth of multiscale structural transformation during comminution.

The scientific novelty of the study lies in the quantitative identification of stage-specific transitions in defect generation mechanisms through the use of complementary diagnostic indicators, the hierarchical reorganization coefficient K_{ier} and the scale redistribution index I_m, which jointly characterize both the change in fracture mechanisms and the depth of multiscale structural transformation of the defect field.

The practical significance of the results consists in identifying structural prerequisites for increased material reactivity, improved mineral liberation, and optimization of comminution and beneficiation regimes in iron quartzite processing.

Conflict of interest

Authors state no conflict of interest.

REFERENCES

1. Brantut, N. (2025), "Semi-brittle flow of rocks: cracks, dislocations and strain hardening", *Proceedings of the Royal Society A*, 481(2307), 20240189. https://doi.org/10.1098/rspa.2024.0189

2. Qin, Z., Li, Y., Han, R., Gao, P. and Cheng, F. (2023), "New insights on the breakage mechanism of magnetite quartzite via high voltage pulse discharge", *Minerals Engineering*, 203, 108297. https://doi.org/10.1016/j.mineng.2023.108297

3. Månbro, C., Broström, M. and Wiklund, J. (2025), "Exploring the role of ore texture in comminution and mineral liberation: A review", *Minerals Engineering*, 230, 109405. https://doi.org/10.1016/j.mineng.2025.109405

4. Wang, X., Ding, J., Ju, F., Xu, N., Xu, Y. and Liu, X. (2024), "Numerical investigation of microcrack growth in heterogeneous granite using boundary element modelling", *Engineering Analysis with Boundary Elements*, 159, pp. 466–484. https://doi.org/10.1016/j.enganabound.2023.12.020

5. Petruk, W. (2000), *Applied Mineralogy in the Mining Industry*. Ottawa: NRC Research Press. https://doi.org/10.4095/215280

6. Shi, Y., Shen, W. and Shao, J. (2025), "Modeling of time-dependent behavior in rocks considering sub-critical microcracking and viscoplastic deformation with a micromechanics-based approach", *Rock Mechanics and Rock Engineering*, 58, pp. 5913–5935. https://doi.org/10.1007/s00603-025-03789-7

7. Lawn, B. (1993), *Fracture of brittle solids*. 2nd edn. Cambridge: Cambridge University Press. https://doi.org/10.1017/CBO9780511623127

8. Paterson, M.S. and Wong, T.-F. (2005), *Experimental Rock Deformation – The Brittle Field*. 2nd edn. Berlin: Springer. https://doi.org/10.1007/b137431

9. Krolop, S., Hartlieb, P., Krietsch, H., Kluge, K. and Gutzmer, J. (2022), "Process mineralogical assessment of the grinding product and liberation characteristics", *Mineral Processing and Extractive Metallurgy Review*, 43(8), pp. 1014–1020. https://doi.org/10.1080/08827508.2021.2023519

10. Zhang, B., Han, R., Gao, P., Yuan, S. and Li, Y. (2025), "Optimization of discharge parameters for high-voltage pulse crushing technology: A review", *Minerals Engineering*, 228, 109356. https://doi.org/10.1016/j.mineng.2025.109356

11. Schönert, K. (1990), "Comminution of mineral raw materials", *Aufbereitungs-Technik*, 31(1), pp. 12–20. https://www.researchgate.net/publication/285725224

12. King, R.P. (2001), *Modeling and Simulation of Mineral Processing Systems*. Oxford: Butterworth-Heinemann. https://www.sciencedirect.com/book/9780750648844

13. Kabemba, A.M., Mutombo, K. and Waters, K.E. (2025), "Towards a dynamic optimisation of comminution circuits under geological uncertainties", *Processes*, 13(2), 443. https://doi.org/10.3390/pr13020443

14. Lieberwirth, H., Duriagina, A. and Klichowicz, M. (2025), "Quantifying the impact of mineral microstructure on the comminution of ores and rocks – A review", *Minerals Engineering*, 234, 109672. https://doi.org/10.1016/j.mineng.2025.109672

15. Peng, J., Du, C., Zhang, F. and Liu, H. (2022), "Fracture and fragmentation of granite specimen under high-voltage pulses", *Geomechanics and Geophysics for Geo-Energy and Geo-Resources*, 8(6), 200. https://doi.org/10.1007/s40948-022-00507-x

16. Tavares, L.M. (2007), "Breakage of single particles: quasi-static", *International Journal of Mineral Processing*, 84(1–4), pp. 15–29. https://doi.org/10.1016/j.minpro.2006.11.002

17. Chen, J., Li, X., Gao, L., Guo, S. and He, F. (2024), "Microwave treatment of minerals and ores: Heating behaviors, applications and future directions", *Minerals*, 14(3), 219. https://doi.org/10.3390/min14030219

18. Ge, X. and Sun, W. (2021), "Acoustic emission characteristics of gabbro after microwave heating", *International Journal of Rock Mechanics and Mining Sciences*, 138, 104616. https://doi.org/10.1016/j.ijrmms.2021.104616

19. Gu, C., Sun, Q., Geng, J., Zhang, Y. and Jia, H. (2024), "Acoustic emission real-time monitoring and analysis of microwave thermal damage of granite", *Environmental Earth Sciences*, 83, 443. https://doi.org/10.1007/s12665-024-11745-5

20. Wills, B.A. and Finch, J.A. (2016), *Wills' Mineral Processing Technology: An Introduction to the Practical Aspects of Ore Treatment and Mineral Recovery*. 8th edn. Oxford: Butterworth-Heinemann. https://doi.org/10.1016/C2013-0-16354-4

21. Kranz, R.L. (1983), "Microcracks in rocks: a review", *Tectonophysics*, 100(1–3), pp. 449–480. https://doi.org/10.1016/0040-1951(83)90198-1

22. Jaeger, J.C., Cook, N.G.W. and Zimmerman, R.W. (2007), *Fundamentals of Rock Mechanics*. 4th edn. Oxford: Blackwell Publishing. https://doi.org/10.1002/9780470758168

23. Petrakis, E., Alexopoulos, I., Pantelaki, O., Karmali, V. and Komnitsas, K. (2025), "Advances in mineral processing of hard-rock lithium ores: A comprehensive review", *Mining, Metallurgy & Exploration*, 42, pp. 1251–1283. https://doi.org/10.1007/s42461-025-01456-9

ЕВОЛЮЦІЯ МІКРОТРІЩИН У ЗАЛІЗИСТИХ КВАРЦИТАХ PR_1SX^1F (НОВОКРИВОРІЗЬКЕ РОДОВИЩЕ) ПІД ЧАС ПОДРОБЛЕННЯ

Ішков В.В., Березняк О.О., Козій Є.С., Пащенко П.С., Козар М.А.

Анотація. Метою дослідження є встановлення закономірностей багатомасштабної ієрархічної перебудови мікротріщинної мережі залізистих кварцитів горизонту PR_1sx^1f у межах повного технологічного циклу дроблення та мокрого кульового подрібнення з кількісною інтерпретацією стадійних змін механізмів дефектогенезу.

Дослідження базується на комплексному петрографічному та кількісному мікроструктурному аналізі зразків залізистих кварцитів, відібраних після послідовних стадій сухого дроблення та мокрого подрібнення. Вимірювання виконувалися за допомогою поляризаційного мікроскопа (Полам Р-312) та інвертованого металографічного мікроскопу (LMM 1400) при фіксованих збільшеннях для забезпечення статистичної надійності результатів. Розраховано інтегральні показники мікротріщинуватості, зокрема коефіцієнт лінійної мікротріщинуватості, коефіцієнт щільності мікротріщин, коефіцієнт ієрархічної перебудови ($K_{ієр}$) та індекс масштабного перерозподілу ($I_м$). Статистичний аналіз розподілів довжин мікротріщин дозволив оцінити зміни їх масштабу та просторової організації.

Результати засвідчили, що еволюція мікротріщинуватості має виражений багаторівневий ієрархічний характер. Монотонне зменшення характерної довжини мікротріщин супроводжується багаторазовим зростанням їх щільності, що відображає перехід від локалізованого росту окремих дефектів до інтенсивної ініціації та взаємодії короткомасштабних мікротріщин. Поетапний аналіз за допомогою коефіцієнта $K_{ієр}$ виявив чергування режимів збалансованого росту та домінування ініціації тріщин, що свідчить про нелінійну перебудову дефектного поля. Квазіекспоненційне зростання індексу $I_м$ підтверджує прогресуючий масштабний перерозподіл дефектів у бік ультракоротких мікротріщин та формування надщільної ієрархічної структури.

Практичне значення результатів полягає у встановленні структурних передумов підвищення реакційної здатності матеріалу та ефективності мінеральної ліберації при збагаченні. Формування густої мережі ультракоротких мікротріщин створює сприятливі умови для розкриття магнетиту в кварцовій матриці та оптимізації режимів подрібнення.

Наукова новизна роботи полягає у кількісному описі стадійних переломів механізмів дефектогенезу та запровадженні взаємодоповнювальних діагностичних індикаторів, що інтегрують локальні переходи з накопичувальним масштабним перерозподілом мікротріщинної системи.

Ключові слова: залізисто-кремниста формація; еволюція мікротріщин; ієрархічна дефектна структура; багатостадійне подрібнення; мінеральна ліберація.